Study of charged particles emitted from ^{117}Te compound nuclei. I. Argon-induced reactions

J. Galin, B. Gatty, D. Guerreau, C. Rousset, U. C. Schlotthauer-Voos,* and X. Tarrago
Laboratoire de Chimie Nucléaire, Institut de Physique Nucléaire, 91406 Orsay, France

(Received 16 July 1973)

The compound nucleus ^{117}Te was formed with ^{40}Ar + ^{77}Se at 71- and 107-MeV excitation energies; the maximum relative angular momenta in the entrance channels are about $70\hbar$ and $110\hbar$. The deexcitation by protons, deuterons, tritons, α particles, and lithium was studied, measuring absolute cross sections, energy spectra, and angular distributions. The experimental results, especially the strong anisotropies of the α-particle angular distributions and the dependence of the average energy on the emission angle, are discussed in terms of the statistical theory and the influence of very high angular momentum on the evaporation mechanism. The angular distributions of the elastic scattering have been measured simultaneously and are described by a strongly absorbing optical potential.

[NUCLEAR REACTIONS ^{nat}Se(^{40}Ar, ^{40}Ar); $E = 146, 201$ MeV; measured $\sigma(\theta)$; optical-model analysis; ^{nat,77}Se(^{40}Ar, p), (^{40}Ar, d), (^{40}Ar, t), (^{40}Ar, α), (^{40}Ar, Li); $E = 146, 201$ MeV; measured $\sigma(E, E_{particle})$, $\sigma(E_{particle}, \theta)$, $\sigma_{particle}$; discussion with regard to statistical model.]

1. INTRODUCTION

Compound-nuclear reactions leading to states in the continuum may be understood by the statistical theory of Weisskopf,[1] based on the independence of the compound-nucleus formation and decay, including, however, a spin-dependent level density.[2,3] Many investigations on energy spectra, absolute cross sections, and excitation functions have supported this concept and have been used to extract level density parameters, the nuclear temperature, and the moment of inertia.[3,4] The angular distributions especially have been shown to be qualitatively related to the spins of the emitting compound-nucleus states.[2,3,5-8]

With the availability of heavy-ion beams, these studies became especially interesting, as heavy-ion-induced reactions involve large relative angular momenta, which allow the population of high spin states in the compound nucleus. Many theoreticians have emphasized the importance of angular momentum in the incident channel,[2,3,9,10] and indeed it was found with reactions induced by ^{12}C, ^{14}N, and ^{16}O[5,9,11,12] that the probability of particle emission depends significantly on the spin of the compound nucleus. Especially the probability of α-particle emission increases strongly with increasing angular momentum as compared to other particles.

These results encourage investigations with even heavier projectiles and consequently higher angular momenta. Under these conditions it should be possible to excite very high spin states, which sometimes might lie near the yrast levels, and to study their deexcitation. The problems involved are relevant for understanding the nature of these states and the reaction mechanism, and they are also important with respect to the formation of new nuclei.

Furthermore the absolute cross sections are of special interest. Liquid-drop-model calculations indicate the existence of a critical angular momentum J_{crit}, above which no complete fusion can occur, corresponding to the maximum possible deformation,[13] or the angular momentum where the fission barrier vanishes.[14,15] These predictions have been qualitatively confirmed by compound-nuclear studies of Bimbot, Lefort, and Vigny[16] by fusion cross-section measurements of Kowalski *et al.*, and Zebelman and Miller,[17] and of Natowitz[18] and direct-reaction cross-section measurements of Pühlhofer and Diamond[19] and Galin *et al.*[20] Problems concerning the absolute values of J_{crit} and its dependence on the nature and energy of the incident nuclei in a compound-nuclear reaction still exist, however. Answers to these questions are very important for the understanding of compound-nucleus formation and decay and are crucial with respect to the formation of exotic nuclei.

In this work, an argon beam was used for the first time for investigations of the evaporation mechanism. The formation of ^{117}Te by ^{40}Ar + ^{77}Se at 146- and 201-MeV incident energies, corresponding to excitation energies of 71 and 107 MeV, respectively, and its decay by emission of protons, deuterons, tritons, α particles, and lithium were studied. Angular distributions, energy spectra, and absolute cross sections have been measured

and are discussed. The incident energies were selected so that at the lower energy the maximum relative angular momentum in the incident channel is in the range which has already been reached by conventional heavy-ion beams (about $70\hbar$), while at the higher incident energy it is larger by about $40\hbar$. To complete the investigations, angular distributions of the elastic scattering have been measured and described by optical-model calculations, in order to determine the distribution of transmission coefficients in the incident channels.

2. EXPERIMENTAL TECHNIQUE

The experiments were performed at the Orsay heavy-ion accelerator ALICE using the $^{40}Ar^{10+}$ beam at 155-MeV energy and the $^{40}Ar^{11+}$ beam at 208 MeV. Beam intensities of 20 nA for the lower energy and 100 nA for the higher energy could be obtained routinely; however, only 20 nA could be used in the experiments because of the fragility of the targets.

The ^{77}Se and ^{nat}Se targets were prepared by evaporation technique as Au-Se-Au sandwiches. The target thicknesses were about 300 $\mu g/cm^2$ for the entrance Au foil, 1 mg/cm^2 for Se, and 800 $\mu g/cm^2$ for the Au backing. Considering the large energy loss of the argon beam, these conditions result in average energies for the Se layer of 201 and 146 MeV, which in this paper are always cited as incident laboratory energies, corresponding to average center-of-mass energies of 132 and 96 MeV, respectively.

No charged particles come from the gold foils, the Coulomb barrier being much greater than the lower energy 146-MeV Ar beam. At 201 MeV, considering the reaction cross sections of Ar on Se and Ar on Au and taking the respective layer thicknesses into account, the ratio of compound nuclei from Au to those from the Se target could be estimated to be lower than 4%. Furthermore most of the compound nuclei from Au undergo fission, so charged-particle emission from Au is negligible as compared to that from the Se target.

As it was the aim to detect simultaneously protons, deuterons, tritons, α particles, and lithium from very low energies to high energies of about 30 MeV for protons and 50 MeV for α particles, a special counter telescope was built, consisting of three transmission mounted fully depleted silicon surface-barrier detectors, E_1 of 45 μm, E_2 of 150 μm, E_3 of 500 μm plus one Si-Li detector E_4 of 4.5-mm thickness. The block diagram of the electronics is shown in Fig. 1. The detector thicknesses were chosen in order to trigger at least one fast coincidence (FC). Particles giving rise to an impulse to FC 1-2 were identified by $E_1 = f(E)$, the others were identified by $E_1 + E_2 = f(E)$, where $E = E_1 + E_2 + E_3 + E_4$. As it is shown on Fig. 2, isotopic separation from this analysis is quite good.

Attention should be paid to the fact that large recoil energies occur in Ar experiments (69 MeV for 201-MeV energy Ar on Se). In the laboratory system, this effect tends to shift the energy spectra to lower energies at backward angles and as a consequence, the low-energy part of the spectrum cannot be analyzed by the coincidence

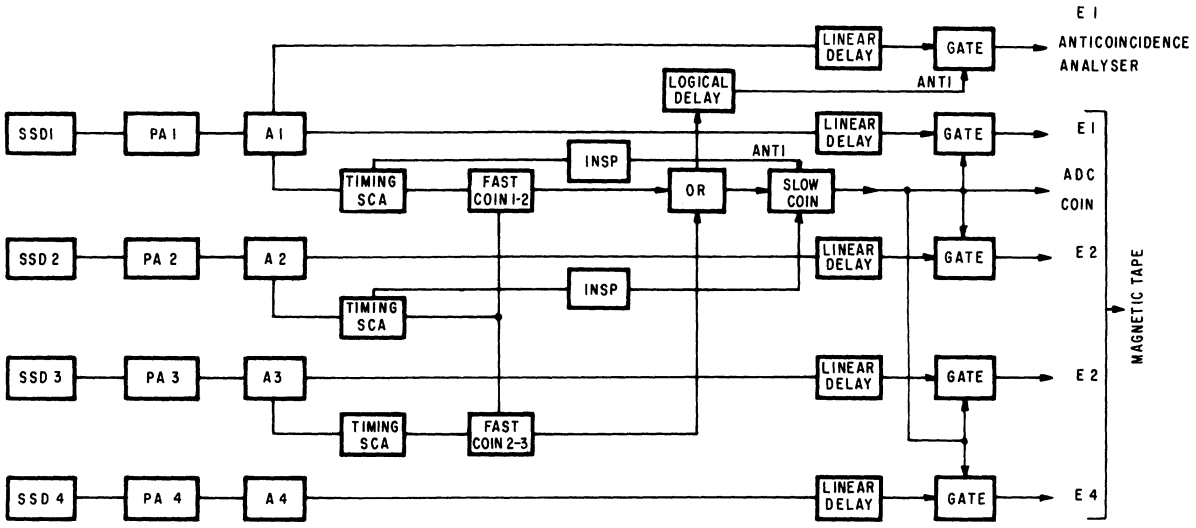

FIG. 1. Block diagram of the electronics.

systems. As protons with $E_p < 2$ MeV and α particles with $E_\alpha < 8$ MeV are stopped in the first detector, and in order to analyze these particles, an anticoincidence (AC) was installed between the counters E_1 and E_2 (A_C1-2). As the laboratory energies of α particles were always larger than 2 MeV, it was easy to separate protons, deuterons, tritons from α particles, but it was not possible indeed to distinguish between these three isotopes of hydrogen. As will be shown afterwards, the deuteron and triton cross sections are much smaller than those for protons; on this low-energy part, we can consider to a good approximation the proton cross sections as being equal to the sum of the measured cross sections for protons, deuterons, and tritons.

Because of the off-line analysis of our experiment, as a control during the run, the E and ΔE impulses of the two detection systems were analyzed directly in two two-dimensional analyzers (64×64 channels). The experimental points in the evaporation measurements were normalized to elastic scattering measurements by a 500-μm-thick monitoring counter placed at a fixed angle. The same counter was used for the measurement of the elastic scattering angular distributions.

Angular distributions of the evaporated particles were measured between $\theta_{lab} = 25-168.5°$ at 146-MeV Ar energy, and $\theta_{lab} = 18-165°$ at 201 MeV (corresponding to $\theta_{c.m.} \approx 25-170°$), with intervals of $\Delta\theta_{lab}$ of 10–15°. The elastic scattering angular distributions were measured in the range from $\theta_{c.m.} = 52-100°$ at the lower energy and from 21.5 to 60° at the higher energy. In order to avoid systematic errors arising from changes in beam position or decomposition of the target, all angular distributions were first measured from forward to backward direction with steps of $2\Delta\theta_{lab}$, then the intermediate points were taken from backward to forward direction.

The high-energy experiment was mainly performed with a natural Se target. It was, however, verified by some measurements on ^{77}Se that the angular distributions and energy spectra are the same, with only the value of the proton cross section being changed.

The beam passing the target was collected in a Faraday cup. For the calculation of the absolute cross sections the mean charge of the argon beam after the target was taken to be 15.3+ at 201 MeV and 14.9+ at 146 MeV resulting from charge measurements by Baron.[21] Target thicknesses were determined by measuring the α-particle energy loss of a ThC(6.06-MeV) and ThC′(8.78-MeV) source and verified by Rutherford scattering at small angles. The solid angle was 0.325 msr. Absolute cross sections are given with errors of ±10% at the higher energy and ±15% at the lower energy.

3. ELASTIC SCATTERING

The angular distributions of the elastic scattering at 146- and 201-MeV incident energies are shown in Fig. 3 together with conventional optical-model calculations. The calculations were performed with the program ABACUS2,[22] using for both the real and imaginary part of the optical potential, a Woods-Saxon form factor. The parameters were found by fitting the higher-energy data and by applying these parameters to the angular distributions at the lower incident energy.

The analysis of the lower-energy data involved some special problems because of the thick target used in the experiment and the corresponding large energy loss of 9 MeV. The experimental cross sections at angles $\theta_{c.m.} > 50°$ are larger by about a factor of 2 to 6 as compared to the cross sections obtained by a simple calculation with the average energy of 146 MeV. Therefore, the target was considered as consisting of six equal pieces, and the optical-model calculations were performed for the six corresponding average energies and later summed. The optical-model description shown in Fig. 3 was calculated in this way.

The optical-model parameters are the same for the two energies (Table I). Parameter set 1 differs slightly from the parameters used by Auerbach and Porter[23] for the description of various elastic scattering cases with projectiles from ^{12}C to ^{16}O and various targets from Al to Au, which had been successfully applied to the elastic scattering of ^{14}N on Ag at 78- and 113-MeV incident energies.[24]

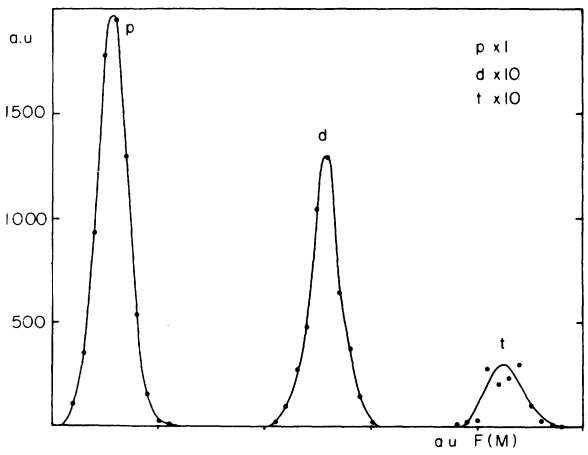

FIG. 2. Mass spectrum.

A similar description was found by slightly changing those optical-model parameters which had been successfully used by the Heidelberg group for much heavy-ion scattering data with projectiles and targets in the mass range $10 \leq A \leq 19$ and for the distorted-wave Born-approximation description of transfer reactions in this region[25] (parameter set 2 in Table I).

As it was the aim to determine by this procedure the transmission coefficients, the results are considered to be satisfactory although some small discrepancies between experiments and calculations are observed. This effect might probably be due to the fact that a part of inelastic scattering could not be separated experimentally from the elastic process.

The resulting angular momentum distribution of the cross sections $\sigma_J/\sum\sigma_J$, where $\sigma_J = \pi\lambda\!\!\!^{-2}(2J+1)\,T_J$ are given in Fig. 4. The T_J are the transmission coefficients and $\lambda\!\!\!^{-}$ is the wavelength of the relative motion. The angular momenta J_0 for which $T_{J0} = \frac{1}{2}$ are $J_0(146\text{ MeV}) = 56\hbar$ and $J_0(201\text{ MeV}) = 93\hbar$, differing by $37\hbar$. The total-reaction cross sections $\sigma_R = \sum_J \sigma_J$ are $\sigma_R(146\text{ MeV}) = 826$ mb and $\sigma_R(201\text{ MeV}) = 1698$ mb.

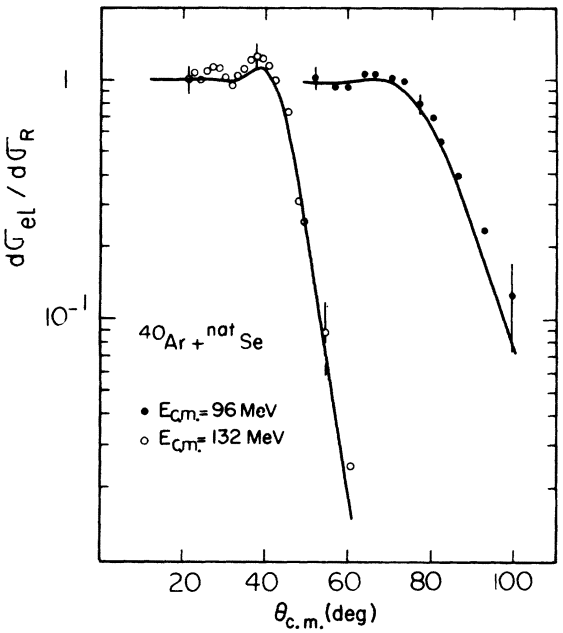

FIG. 3. Angular distributions of the elastic scattering Ar on ^{nat}Se with optical-model descriptions (parameter set 1 in Table I).

4. COMPOUND-NUCLEUS RESULTS

A. Charged-particle spectra

Energy spectra in the center-of-mas system of the detected protons and α particles at both incident energies and of deuterons and tritons at the higher incident energy are presented in Figs. 5–9.

As the center-of-mass angle at a given laboratory angle varies with the kinetic energy of the emitted particle, the experimental center-of-mass angles are in reality average values obtained by

$$\bar{\theta}_{\text{c.m.}} = \frac{\int \sigma(E_\nu)\theta_{\text{c.m.}}(E_\nu)\,dE_\nu}{\int \sigma(E_\nu)\,dE_\nu},$$

where σ denotes the differential cross section for a particle with energy E_ν and the corresponding center-of-mass angle $\theta_{\text{c.m.}}(E)$. By comparing $\bar{\theta}_{\text{c.m.}}$ to the center-of-mass angles of the kinetic energies, which correspond to the half-width of the spectra, the angular uncertainties were found to be very small, as demonstrated later with the total angular distributions (Figs. 11 and 12). For simplicity in the text $\bar{\theta}_{\text{c.m.}}$ is called $\theta_{\text{c.m.}}$.

The energy spectra exhibit the typical form of evaporation spectra. For α particles, the maximum energy values depend significantly on the emission angle, while this effect is less pronounced for protons. To investigate this dependence the average kinetic energy of the α particles at the higher bombarding energy versus the emission angle is plotted in Fig. 10. A correction has been applied to take into account the mean energy

TABLE I. Optical-model parameters for the description of the elastic scattering Ar on ^{nat}Se at $E_{\text{c.m.}} = 96$ MeV and $E_{\text{c.m.}} = 132$ MeV (Fig. 3); for definitions, see text.

Set No.	U_0 (MeV)	r_{0_R} (fm)	a_R (fm)	W_0 (MeV)	r_{0_I} (fm)	a_I (fm)
1	41.8	1.20	0.45	16.4	1.31	0.44
2	100	1.185	0.48	30	1.37	0.26

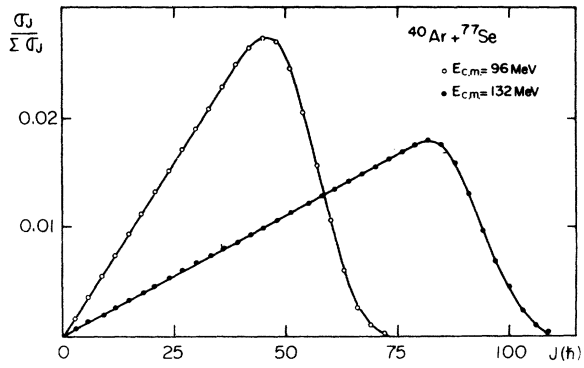

FIG. 4. Angular momentum distribution of the cross-sections $\sigma_J/\sum\sigma_J$ (parameter set 1 in Table I).

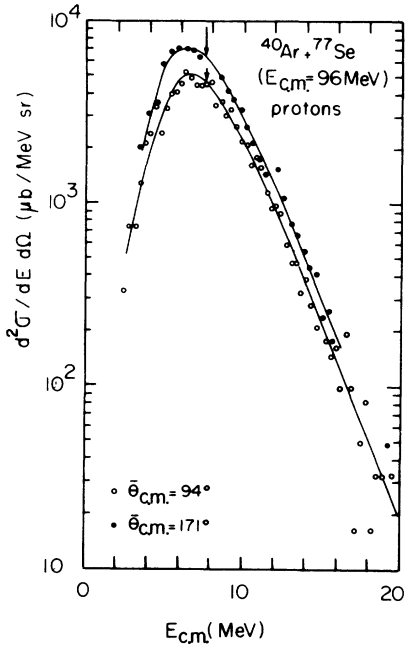

FIG. 5. Center-of-mass energy spectra of the evaporated protons; the solid lines are to guide the eye; the arrows indicate the average energies.

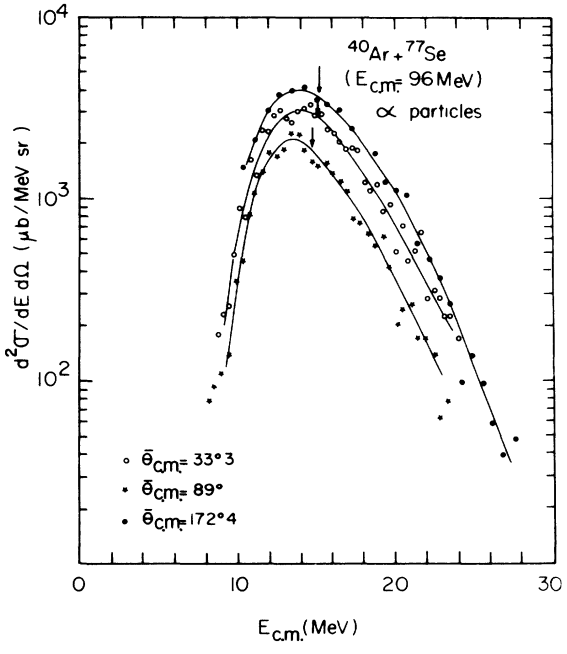

FIG. 6. Center-of-mass energy spectra of the evaporated α particles; the solid lines are to guide the eye; the arrows indicate the average energies.

loss of α particles in the target. The uncertainty on the experimental points, mainly due to the instability of the linear electronics chain, is about ±200 keV. An anisotropic distribution, symmetrical around $\theta_{c.m.} = 90°$ is found. This behavior, already predicted by Ericson with statistical model calculations[2] for cases involving high spins in the compound nucleus, has never been verified experimentally until now. Indeed, as angular momentum has only slight influence on the average kinetic energies, the observed effect can only be detected experimentally when very high spin states in the compound nucleus are populated.

For α particles at the lower energy and protons at both bombarding energies the average kinetic energies are found, within the experimental errors, to be independent of emission angle. This result indicates that the spins of the compound-nuclear states are larger at the higher excitation energy and that the influence of angular momentum in α-particle emission is more pronounced than in proton evaporation.

B. Angular distributions

Angular distributions integrated over particle energies for protons, deuterons, tritons, and α particles at both incident energies are presented in Figs. 11 and 12. Attention should be paid to the fact that the measurements at the higher excitation energy were mainly performed with a natural Se target. The angular distributions and the absolute cross sections shown in Fig. 12 were obtained

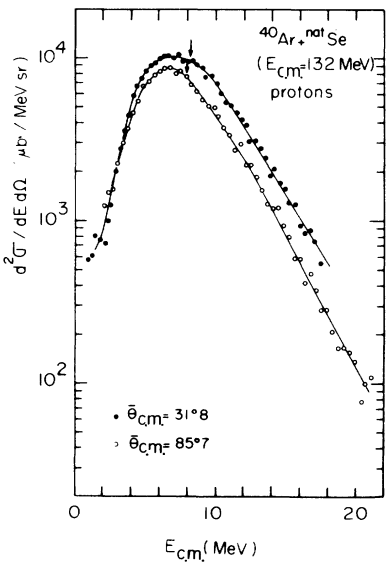

FIG. 7. Center-of-mass energy spectra of the evaporated protons; the solid lines are to guide the eye; the arrows indicate the average energies.

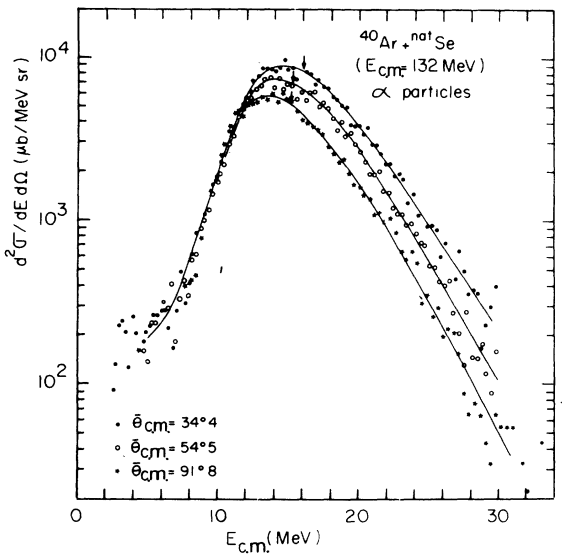

FIG. 8. Center-of-mass energy spectra of the evaporated α particles; the solid lines are to guide the eye; the arrows indicate the average energies.

in this way. However, it was verified by measurements on a ^{77}Se target at several angles that the form of the angular distributions as well as of the energy spectra are the same for natural Se and ^{77}Se. Even the absolute cross sections for α particles, deuterons, and tritons are the same; only the proton cross section for the ^{77}Se target is larger by a factor 1.24. This factor has to be considered when the absolute values in Fig. 12 are compared.

Very good statistics allow us to present also the angular distributions of deuterons at both excitation energies and of tritons at the higher energy despite the small cross sections of about 1 mb. However, as deuterons and tritons could not be distinguished from protons for laboratory energies smaller than 2 MeV the angular distributions shown are only integrated over center-of-mass particle energies greater than about 8 MeV.

The lines in Figs. 11 and 12 are least-squares fits to the data with a sum over even Legendre polynomials in order to extract values of the anisotropies $\sigma_{0°}/\sigma_{90°}$ given in Table II.

The angular distributions are symmetric around $\theta_{c.m.} = 90°$. Normally in heavy-ion induced (C, N, O, Ne) compound-nuclear reactions at sufficiently high excitation energies, the angular distributions of charged particles and especially α particles are asymmetric[5,10,12] with a strongly peaked component in the forward direction. This effect has been explained by contributions from direct interactions, which may impose severe difficulties on the compound-nuclear studies, whenever the direct reactions are still significant at angles near 90°. In the present study the direct contributions are negligible within the experimental errors.

The dependence of the angular distributions upon particle energy is demonstrated in Figs. 13–16, where proton and α angular distributions integrated over small energy ranges are presented. Again the full lines are least-squares fits. The corresponding anisotropies $\sigma_{0°}/\sigma_{90°}$ are given in Table III.

C. Cross sections

The absolute cross sections integrated over all angles and particle energies for the emission of protons, deuterons, tritons, α particles, and lithium from the compound nucleus formed by $^{40}Ar + ^{77}Se$ at both excitation energies are given in Table IV. To obtain the absolute cross sections

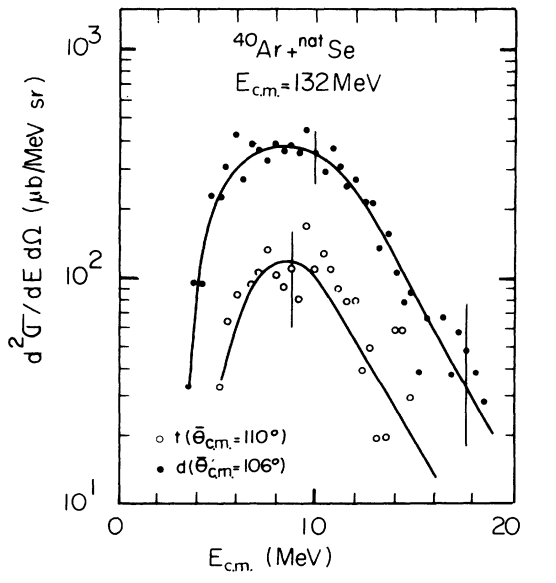

FIG. 9. Center-of-mass energy spectra of the evaporated deuterons and tritons; the solid lines are to guide the eye.

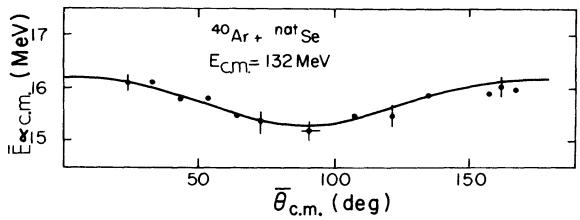

FIG. 10. Angular dependence of the average kinetic energy $\bar{E}_\alpha$ of the α-particle spectra at 132-MeV center-of-mass energy.

TABLE II. Anisotropies $\sigma_{0°}/\sigma_{90°}$ of the total proton, deuteron, triton, and α-particle angular distributions (Figs. 11 and 12).

	P	$d(E_{c.m.}>8$ MeV)	$t(E_{c.m.}>10$ MeV)	α
$E_{c.m.}=132$ MeV	1.53 ± 0.11	1.62 ± 0.15	2.60 ± 0.50	3.16 ± 0.15
$E_{c.m.}=96$ MeV	1.43 ± 0.10	1.67 ± 0.30		2.53 ± 0.20

for deuteron and triton evaporation, some corrections were considered in order to take the particles with energies below the detection threshold of the first coincidence into account. The probability of triton and α-particle emission is found to increase significantly with excitation energy as compared to that of proton evaporation.

Some problems are also involved in the lithium cross sections. Because of the large recoil energy of the compound-nucleus complete lithium spectra could be obtained only in the very forward direction. To get an idea of the absolute cross section, at the higher energy an isotropic angular distribution determined by the value measured at $\theta_{c.m.}=20°$ was assumed. Thus the value in Table IV has to be considered as an upper limit. At the lower energy no lithium was observed. The upper limit of the cross section shown in Table IV, is therefore the cross section for a single event.

5. DISCUSSION

In order to illuminate the process of compound-nucleus formation and decay in the case of very high angular momentum the discussion is focused on some very special problems: the angular distributions of the high-energy particles arising only from the first evaporation step, the anisotropies, and the dependence of the evaporation mechanism on the compound-nucleus spin.

A. Theoretical aspects

The evaporation of particles in a compound-nuclear reaction can be interpreted by the semiclassical statistical theory of Ericson[2] whenever the spin of the incident particle is small as compared to the spin of the formed compound-nucleus state, a condition which is certainly well fulfilled in the present reaction. The probability for the emission of particle ν with the energy E_ν and spin s_ν in the direction of the angle θ is given by

$$\sigma(\theta,E_\nu)\propto\int_0^\infty 2JT_J\,dJ\,\frac{1}{\Gamma_J}\,(2s_\nu+1)\rho(E_{x\nu},0)\int_0^\infty 2lT_l^{(\nu)}\exp\left[-\left(\frac{J^2+l^2}{2\sigma_\nu{}^2}\right)\right]J_0\left(\frac{iJl}{\sigma_\nu{}^2}\right)W_{Jl}(\theta,E_\nu)\,dl, \tag{1}$$

where the angular dependence is described by:

$$W_{Jl}(\theta,E_\nu)=\frac{1}{4\pi}\left[j_0\left(\frac{iJl}{\sigma_\nu{}^2}\right)\right]^{-1}\sum_k(-)^k(4k+1)\left[\frac{(2k)!}{(2^k k!)^2}\right]^2 j_{2k}\left(\frac{iJl}{\sigma_\nu{}^2}\right)P_{2k}(\cos\theta). \tag{2}$$

T_J and T_l are the transmission coefficients in the entrance and exit channels, J and l are the spin of the compound-nucleus state and the angular momentum of the emitted particle, respectively, Γ_J is the total decay width, j_{2k} are spherical Bessel functions, and P_{2k} are Legendre polynomials.

The level density for the residual nucleus at the excitation energy $E_{x\nu}$ and spin J is denoted by $\rho(E_{x\nu},J)$. Lang[26] and Thomas[3] have shown that the density of states with energy E and spin projection M is given by

$$\omega(E,M)=B\,\frac{\exp\{2[a(E-M^2\hbar^2/2\mathcal{I})]^{1/2}\}}{a^{3/2}t^3}, \tag{3}$$

where B is a constant depending on the moment of inertia $\mathcal{I}$ of the nucleus under consideration, a is the level density parameter, t is the nuclear temperature, which is related to the excitation

TABLE III. Anisotropies $\sigma_{0°}/\sigma_{90°}$ of proton and α-particle angular distributions integrated over small ranges of the particles' kinetic energies. The uncertainties are in the order of 15–20% (Figs. 13–16).

	Protons				α particles				
	4–6 MeV	6–8 MeV	8–10 MeV	10–13 MeV	10–15 MeV	15–20 MeV	20–25 MeV	25–30 MeV	>30 MeV
$E_{c.m.}=132$ MeV	1.60	1.45	1.44	1.47	2.78	3.64	4.08	4.53	4.60
$E_{c.m.}=96$ MeV	1.58	1.51	1.28	1.48	2.01	3.26	4.24		

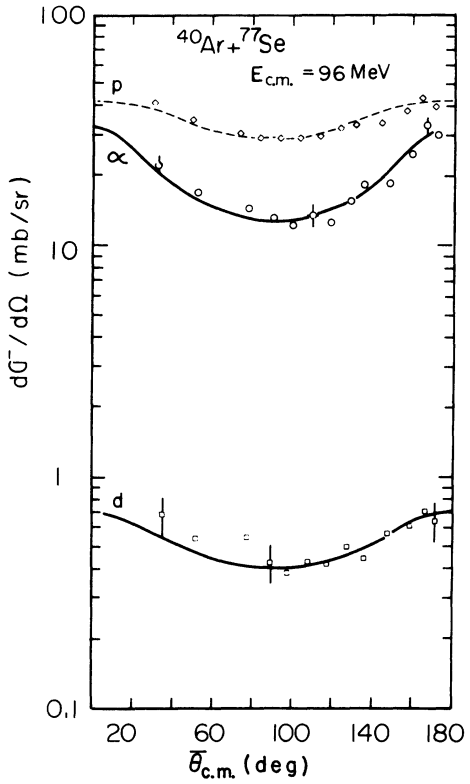

FIG. 11. Angular distributions of protons and α particles integrated over the total spectra and of deuterons integrated above 8 MeV; the solid lines are least-squares fits with a sum of even Legendre polynomials. For definition of the angular uncertainties see text; at the lower energy they are included in the points.

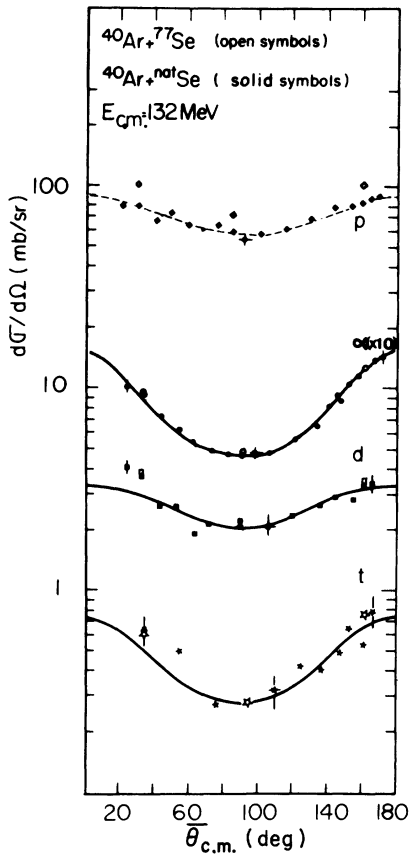

FIG. 12. Angular distributions of protons and α particles integrated over the total spectra and of deuterons and tritons integrated above 8 MeV; the solid lines are least-squares fits with a sum of even Legendre polynomials. For definition of the angular uncertainties see text; at the lower energy they are included in the points.

energy E by

$$E = at^2 - \tfrac{3}{2}t + \frac{M^2\hbar^2}{2\mathcal{I}} \tag{4}$$

and the spin cutoff parameter is defined as usual by $\sigma_\nu^2 = \mathcal{I}t/\hbar^2$.

The level density for levels with spin J is then obtained by

$$\rho(E,J) = \omega(E, M=J) - \omega(E, M=J+1)\,. \tag{5}$$

A Taylor series expansion of $\ln\omega(E,M)$ leads to an expression which in the limit of not too high spins is the same as the conventional one, used for the deduction of Eqs. (1) and (2). It was verified for the present studies that in the angular momentum regions under consideration, the limiting expression of the level density gives the same results within the experimental errors as the exact one.

From Eq. (2), it follows immediately that the anisotropy of the angular distributions is mainly determined by Jl/σ_ν^2 increasing with J and l, but decreasing slowly with increasing excitation ener-

TABLE IV. Absolute cross sections integrated over angles and particle energies for the emission of protons, deuterons, tritons, α particles, and lithium.

		P (mb)	d (mb)	t (mb)	α (mb)	Li (mb)
$E_{c.m.}$ = 132 MeV	^{nat}Se	880 ± 90	47 ± 10	15 ± 5	840 ± 90	<1
	^{77}Se	1090 ± 110	47 ± 10	15 ± 5	840 ± 90	<1
$E_{c.m.}$ = 96 MeV	^{77}Se	410 ± 60	8.5 ± 1.5	1.5 ± 0.7	207 ± 30	<0.1

gy of the residual nucleus. Thus strong anisotropies are the indication of particles emitted with high energy and large angular momentum by a high spin state of the compound nucleus.

Two cases may be distinguished:

(a) weak coupling, when $Jl/\sigma_\nu^2 \ll 1$, resulting in the extreme case in a spin-independent level density which gives isotropic angular distributions. More generally the average angular distribution is given by

$$\sigma(\theta)\alpha 1 + \tfrac{1}{3} m_\nu \frac{R^2\hbar^2\bar{J}^2}{2\mathcal{J}^2 t} P_2(\cos\theta), \tag{6}$$

where m_ν is the mass of the emitted particle and R the nuclear radius. This method has been normally used to extract the average spin of the compound nucleus.[11,12]

(b) strong coupling, when $Jl/\sigma_\nu^2 \gg 1$, which in the extreme case means complete alignment of $\vec{J}$ and $\vec{l}$ and gives as average angular distribution

$$\sigma(\theta)\alpha(1/\sin\theta). \tag{7}$$

In less extreme cases no simple approximation is possible and Eq. (1) has to be applied.

All reactions which until now have been discussed in the literature are predominantly of type (a); nevertheless in some less extreme cases the complete formula (1) has been applied.[7,27] An estimate for the first steps of the evaporation chains shows, however, that in the present work, the reaction is mainly of type (b) with $\sigma_\nu^2 \sim 10^{+2}$; as will be shown in Sec. B, it is found that $J_{\max} \geq 70\hbar$ and $50\hbar$ at the higher and lower excitation energies, respectively, and $l_{p\max} \sim 20\hbar$, $l_{\alpha\max} \sim 25\hbar$. Indeed, as an example the total α-particle angular distribution resulting from the high excitation energy may be well described by expression (7) except for very large (and small) angles (Fig. 17).

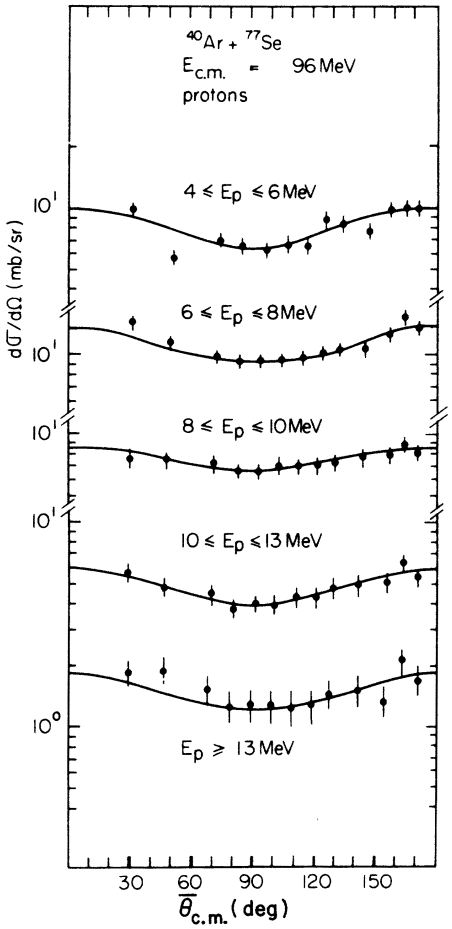

FIG. 13. Proton angular distributions integrated over small ranges of the particles' kinetic energies; the solid lines are least-squares fits with a sum over Legendre polynomials.

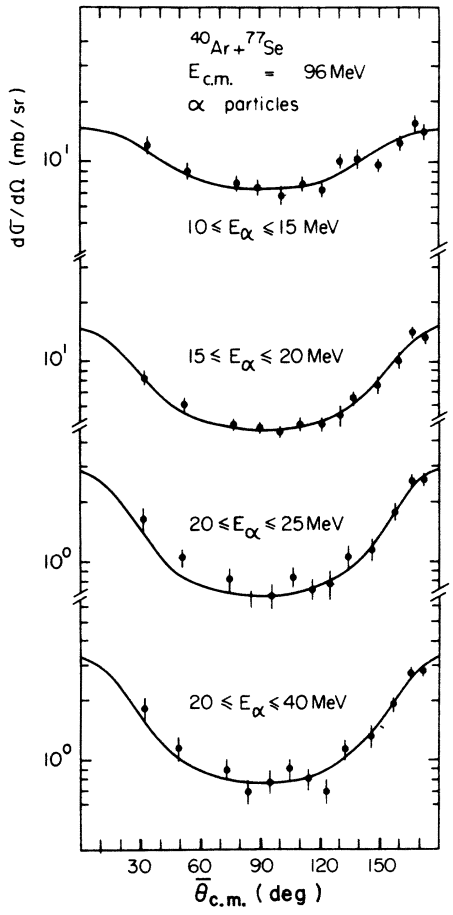

FIG. 14. α-particle angular distributions integrated over small ranges of the particles' kinetic energies; the solid lines are least-squares fits with a sum over Legendre polynomials.

B. Description of the angular distributions

The experimentally observed charged particles arise from a whole evaporation cascade. A description of their angular distributions would imply a complete calculation of each evaporation step at all angles, project which had to be given up because of the long calculation time. However, it was found by a comparison of calculated first step and experimental spectra, that α particles with $E_\alpha \geq 25$ MeV and protons with $E_p \geq 13$ MeV are predominantly due to the first evaporation steps. So, the presented theory describing the first step of the evaporation chains can be only applied to these high-energy particles.

Therefore angular distribution calculations were performed according to (1) with the average energies of the energy regions given above. The free parameters of the theory were chosen to be: $\mathcal{I} = \mathcal{I}_{rig}$, the moment of inertia of a rigid body; $a = A/8$, where A is the mass number of the nucleus under consideration. The level density parameter a was adjusted according to the average value given in the literature. Results of Brun *et al.*[12] indicate that in the mass region under consideration $a = A/6$ should be more appropriate. Calculations were performed with this value giving, however, only slightly stronger anisotropies. With respect to the average moment of inertia, the nuclei of the incident channel should have the tendency in the present reaction to form a compound nucleus with oblate deformation rather than with prolate one.[14] With $a = A/6$ a value of $\mathcal{I}/\mathcal{I}_{rig} = 1.2$ is still compatible with the experimental angular distributions. Thus a choice of $\mathcal{I} = \mathcal{I}_{rig}$ seems to be physically reasonable within the experimental errors.

As shown by the previous discussion of Eq. (2) the angular distributions depend significantly on the population distributions of the compound nucleus, and the anisotropies are expected to increase with the spin of the compound-nuclear states. On

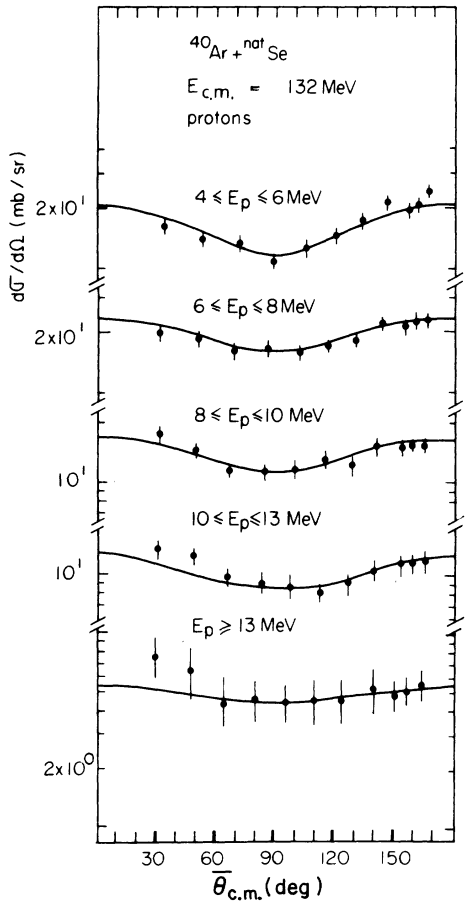

FIG. 15. Proton angular distributions integrated over small ranges of the particles' kinetic energies; the solid lines are least-squares fits with a sum over Legendre polynomials.

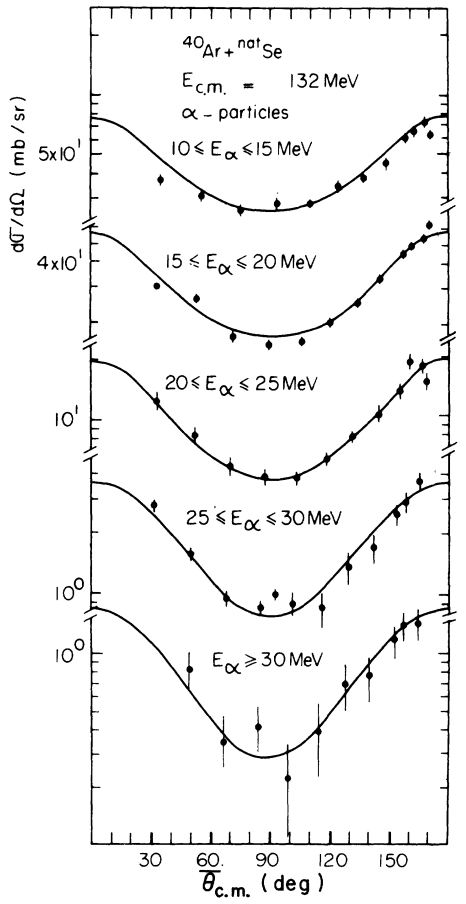

FIG. 16. α-particle angular distributions integrated over small ranges of the particles' kinetic energies; the solid lines are least-squares fits with a sum over Legendre polynomials.

the other hand liquid-drop-model calculations[13,14] and different experiments[15-20] indicate the existence of a critical relative angular momentum J_{crit}, above which two nuclei can no longer form a compound nucleus. From the empirical dependence, earlier given by Natowitz[12] the J_{crit} for a compound nucleus of mass 117 is expected to be $J_{crit} \sim 52\hbar$. Recent measurements have, however, shown, that the value of J_{crit} is not uniquely determined by the compound nucleus under consideration, but increases with heavier projectiles in the entrance channel[17] and higher excitation energies.[18]

Thus one should determine by a description of the angular distributions the population distribution of the compound nucleus, and possibly the J_{crit} for compound-nucleus formation. In order to investigate this effect quantitatively, calculations for the angular distributions were performed with different "cutoff values" J_{co} in the angular momentum distribution of the entrance channel (Figs. 18 and 19). For α particles the anisotropies become significantly larger with increasing angular momentum cutoff, remain, however, approximately the same for values of $J_{co} \gtrsim 52\hbar$ and $J_{co} \gtrsim 72\hbar$ at the low and high excitation energies, respectively. As will be shown in the next section this effect is interpreted to be due to yrast levels.

From the calculations presented it can be concluded that the population distribution of the compound nucleus giving the observed angular distributions are certainly different at the two excitation energies. At 71-MeV levels with spins at least up to $50\hbar$, and at 107-MeV levels with spins at least up to $70\hbar$, have to be taken into account. However, the existence of a critical angular momentum for compound nucleus formation J_{crit} cannot be proved by this analysis. It is only found, that, if J_{crit} exists, it will be $J_{crit} \gtrsim 50\hbar$ at 71 MeV and $J_{crit} \gtrsim 70\hbar$ for 107 MeV.

C. Evaporation mechanism

Even without more detailed calculations, which would have to take into account the whole evaporation chain, it is possible to get some qualitative ideas of the evaporation mechanism.

As shown, the maximum spin of the compound nucleus at the higher excitation energy is certainly larger than at the lower energy. The strong influence of angular momentum on α-particle evaporation is demonstrated by the variation of the average kinetic energies with the emission angle. The same effect is indicated by the measurement of the absolute cross sections with the incident energy.

Further information may be obtained by the anisotropies of the angular distributions (Table II). The total α-particle angular distributions are much more anisotropic at the higher excitation energy, whereas the proton angular distributions exhibit the same anisotropies at both excitation energies. Again the influence of the compound-nucleus spin is only significant on α-particle emission.

The anisotropies for proton emission at both excitation energies are found to be constant within the experimental errors at all proton energies (Figs. 13 and 14, Table III). However, for α particles the anisotropy increases significantly with the kinetic energy of the emitted particles, approaching some constant value at the highest α-particle energies (Figs. 15 and 16, Table III). A

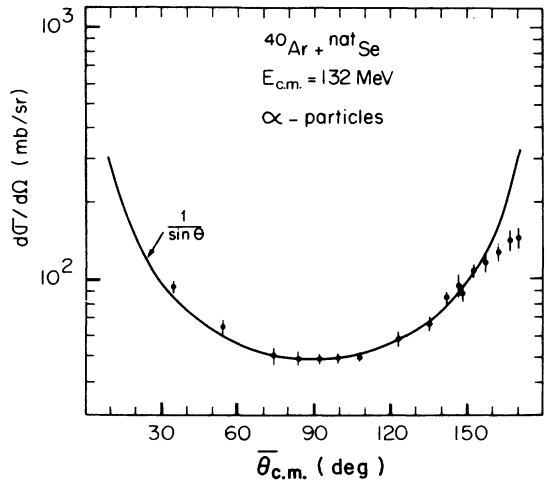

FIG. 17. Total α-particle angular distribution at $E_{c.m.} = 132$ MeV compared with the prediction of the statistical theory in the strong coupling limit, formula (7).

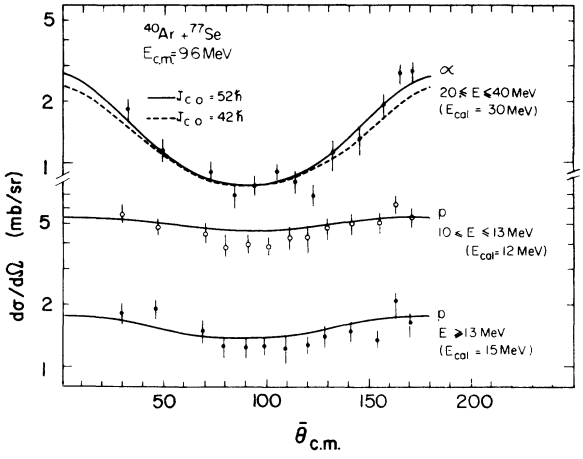

FIG. 18. Predictions of angular distributions with the statistical theory for the first step emission of protons and α particles with different "angular momentum cutoff" in the entrance channel J_{co}.

similar increase of the α-particle anisotropies has been observed by Reedy *et al.*[11] in evaporation experiments from the compound nucleus ^{75}Br formed in different heavy-ion reactions. For protons the anisotropies show a slightly decreasing tendency with particle energy. These effects indicate that high spin states favor the emission of high-energy α particles. The same interpretation has to be applied to the present case. This explanation is further supported by results of Williams and Thomas[28] who have calculated that the average kinetic energy of the evaporated α particles increases significantly with compound-nucleus spin, while it is constant for protons.

Attention has, however, to be paid to the fact, that for the present reaction the anisotropies for α particles approach some constant value. Furthermore, calculations of the angular distributions of high-energy α particles with different J_{co} values have shown, that from a certain value of J_{co} the anisotropies remain approximately constant.

To illustrate this point Fig. 20 shows how the cross section for the emission of α particles with a definite energy depends on the compound-nucleus spin. It is found, that this probability distribution has a maximum and that the corresponding compound-nucleus spin increases with the α-particle energy, but decreases again for very high-energy α particles. Thus, high spin states of the compound nucleus favor the emission of α particles with large energies; however, for states near the yrast line, high-energy α particles are defavored and give way to low-energy α particles.

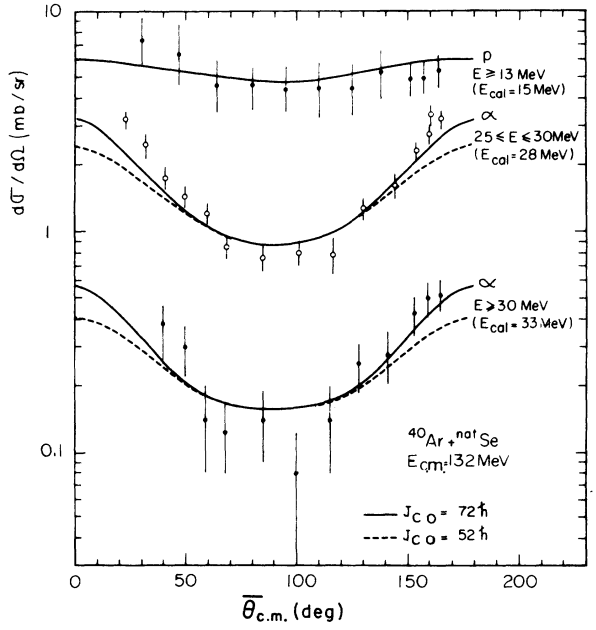

FIG. 19. Predictions of angular distributions with the statistical theory for the first step emission of protons and α particles with different "angular momentum cutoff" in the entrance channel J_{co}.

6. CONCLUSIONS

The present studies of the reactions of Ar on Se demonstrate the significant influence of angular momentum on the formation and deexcitation of compound nuclei, manifesting itself especially in the very anisotropic emission of the evaporated particles. It is shown, that the larger compound-nucleus spins are reached at the high excitation energy. Mainly the evaporation of α particles is affected by the angular momentum and as a consequence a high spin of the compound nucleus favors the emission of high-energy α particles. In this sense the earlier results, found with lighter projectiles and smaller angular momenta, may be extrapolated to the region of very high spin states in the compound nucleus. However, the emission probability for high-energy α particles decreases remarkably at states near the yrast line.

The predictions of the statistical theory are well fulfilled. For the first time a dependence of the average energy on the emission angle could be experimentally verified. Furthermore the angular distributions show complete symmetry with regard to $\theta_{c.m.} = 90°$, in contrast to earlier studies of heavy-ion-induced compound-nuclear reactions, where generally the symmetry about 90° had been destroyed by a strongly forward-peaked component. In this sense, Ar or similar projectiles are more appropriate for compound-nuclear studies than are lighter ones.

The angular distributions of the high-energy par-

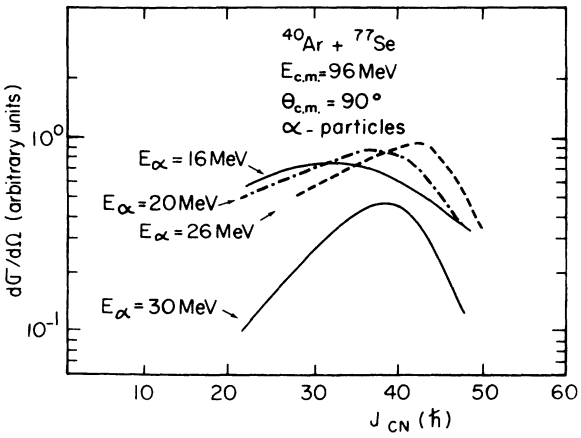

FIG. 20. Dependence on the compound-nucleus spin of the cross section for the emission of α particles with a definite kinetic energy E_α.

ticles are well reproduced by statistical model calculations and allow the determination of the compound-nucleus population distributions.

For more detailed information the same compound nucleus, formed at both excitation energies by the reactions of ^{14}N on ^{103}Rh, has been investigated. Again the deexcitation by protons, deuterons, tritons, α particles, and lithium was studied. The results will be compared to the reactions of ^{40}Ar with Se in the following publication.[29]

The authors want to thank Professor M. Lefort for his continuous interest in this work, his support, and many helpful discussions. A critical reading of the manuscript by Dr. R. L. Hahn is gratefully acknowledged.

---

*On leave of absence from Physikalisches Institut der Universität, Marburg, Germany, supported by G. S. I., Darmstadt, Germany.

[1]V. F. Weisskopf, Phys. Rev. 52, 295 (1937); J. M. Blatt and V. F. Weisskopf, *Theoretical Nuclear Physics* (Wiley, New York, 1952), p. 367.

[2]T. Ericson and V. Strutinsky, Nucl. Phys. 8, 284 (1958); 9, 689 (1959); T. Ericson, Advan. Phys. 9, 425 (1960).

[3]T. D. Thomas, Annu. Rev. Nucl. Sci. 18, 343 (1968), and references therein.

[4]C. C. Lu, L. C. Vaz, and J. R. Huizenga, Nucl. Phys. A190, 229 (1972); A197, 321 (1972).

[5]W. J. Knox, A. R. Quinton, and C. E. Anderson, Phys. Rev. 120, 2120 (1960); H. C. Britt and A. R. Quinton, *ibid.* 124, 877 (1961).

[6]C. E. Hunting, Phys. Rev. 123, 606 (1961).

[7]F. E. Durham and M. L. Halbert, Phys. Rev. 137, 850 (1965).

[8]J. Benveniste, G. Merkel, and A. Mitchell, Phys. Rev. 174, 1357 (1968).

[9]D. Sperber, Phys. Rev. 151, 788 (1966).

[10]J. R. Grover and J. Gilat, Phys. Rev. 157, 802 (1967); J. Gilat and J. R. Grover, Phys. Rev. C 3, 734 (1971).

[11]R. C. Reedy, M. J. Fluss, G. F. Herzog, L. Kowalski, and J. M. Miller, Phys. Rev. 188, 1771 (1969).

[12]C. Brun, B. Gatty, M. Lefort, and X. Tarrago, Nucl. Phys. A116, 177 (1968).

[13]B. N. Kalinkin and I. Z. Petkov, Acta Phys. Polon. 25, 265 (1964).

[14]S. Cohen, F. Plasil, and W. J. Swiatecki, in *Proceedings of the Third Conference on Reactions between Complex Nuclei,* edited by A. Ghiorso, R. Diamond, and H. Conzett (Univ. of California Press, Berkeley and Los Angeles, 1963), p. 325.

[15]M. Blann and F. Plasil, Phys. Rev. Lett. 29, 303 (1972).

[16]R. Bimbot, M. Lefort, and A. Vigny, J. Phys. (Paris) 29, 563 (1968).

[17]L. Kowalski, J. G. Jodogne, and J. M. Miller, Phys. Rev. 169, 894 (1968); A. M. Zebelman and J. M. Miller, Phys. Rev. Lett. 30, 27 (1973).

[18]J. B. Natowitz, Phys. Rev. C 1, 623 (1970); J. B. Natowitz, E. T. Chulick, and M. N. Namboodiri, *ibid.* 6, 2133 (1972).

[19]F. Pühlhofer and R. M. Diamond, Nucl. Phys. A191, 561 (1972).

[20]J. Galin, D. Guerreau, M. Lefort, and X. Tarrago, J. Phys. 32, 7 (1971).

[21]E. Baron, private communication.

[22]E. H. Auerbach, BNL Report ABACUS 2 (unpublished), modified program by B. Donnelly and H. C. Chow.

[23]E. H. Auerbach and C. E. Porter, in *Proceedings of the Third Conference on Reactions between Complex Nuclei* (See Ref. 14), p. 19.

[24]J. Galin, D. Guerreau, and X. Tarrago, unpublished results.

[25]U. C. Voos, W. von Oertzen, and R. Bock, Nucl. Phys. 135, 207 (1969); U. C. Schlotthauer-Voos, H. G. Bohlen, W. von Oertzen, and R. Bock, Nucl. Phys. A180, 385 (1972); U. C. Schlotthauer-Voos, R. Bock, H. G. Bohlen, H. H. Gutbrod, and W. von Oertzen, Nucl. Phys. A186, 225 (1972).

[26]D. W. Lang, Nucl. Phys. 77, 545 (1966).

[27]D. V. Reames, Phys. Rev. 137, 332 (1965).

[28]D. C. Williams and T. D. Thomas, Nucl. Phys. A92, 1 (1967).

[29]J. Galin, B. Gatty, D. Guerreau, C. Rousset, U. C. Schlotthauer-Voos, and X. Tarrago, following paper, Phys. Rev. C 9, 1126 (1974).